Antimicrobial activity of Rare Earth Metal doped ZnO Thin Films prepared by Low Cost Spray Technique against Fish pathogens

R. Balaji[1], N. Jabena Begum[2], P. Seenuvasakumaran[3*], R. Anandhi[4], K. Saravanakumar[5], A. Vinodhini[6], K. Saravanan[1], A. Ubaithulla Baig[7]

[1]PG & Research Department of Physics, Muthurangam Government Arts College (Auto), Vellore-632002.

[2]Department of Physics, DKM College for Women (Autonomous), Vellore-632001.

[3]Department of Physics, Government Arts & Science College, Tirupattur- 635901.*

[4]Department of Physics, Periyar Maniyammai University, Thanjavur- 613403

[5]Department of Physics, Mahendra Institute of Technology (Autonomous), Namakkal (DT)-637503.

[6]PG & Research Department of Zoology, DKM College for Women (Autonomous), Vellore-632001.

[7]Department of Physics, C. Abdul Hakeem College of Engineering and Technology, Ranipet – 632509.

Corresponding Author

Dr. P. Seenuvasakumaran

Principal

Department of Physics, Government Arts & Science College, Tirupattur - 635901.

Contact No: 9443541802

Email: rpyeskay@gmail.com

ABSTRACT

Public health is at risk due to the global problem of antibiotic resistance. As the genes for antibiotic resistance can be passed across bacteria in humans, animals, and aquatic species, the overuse of antibiotics leads to the aforementioned issue. The extensive use of antibiotics in aquaculture has a number of negative effects on both the industry and the health of consumers. Because of their antibacterial action and minimal toxicity, ZnO-based nanoparticles in future may replace some conventional antibiotics. This study's objectives is to test the antibacterial activities of yttrium-doped zinc oxide (ZnO:Y) nanoparticles against certain significant fish pathogens. In the current work, undoped and Yttrium (2, 4 and 6 at %) doped ZnO thin films were prepared by simplified Spray pyrolysis technique to evaluate their antimicrobial efficacy against certain fish pathogens like Aeromonas hydrophila, Salmonella enterica, Lactococcus garvieae and Streptococcus agalactiae. The structural, morphological and optical properties of synthesized samples were examined.

A well-arranged crystallite hexagonal wurzite structure was revealed by XRD spectra. The undoped ZnO and ZnO:Y films show the average transmittance of 75 % in 600 to 1200 nm wavelength region. The uniformly distributed, spherical-shaped grains were observed in SEM for undoped ZnO whereas a tetra pod chain like structure with an enhanced surface to volume ratio was observed for 4 at.% of yttrium doped ZnO thin films. From the antibacterial screening study, even though the entire Y doped films (2, 4, 6 at. % of Y) was identified having potent antibacterial activity, the 4 at. % of Y doped ZnO sample exhibited the maximum activity against the examined pathogens. The current results indicate that the degree of zone of inhibition was more against gram negative bacterial strains Aeromonas hydrophila, Salmonella enterica when compared to the gram positive bacteria Lactococcus garvieae and Streptococcus agalactiae.

Keywords: *Zinc Oxide thin films, Fish Pathogens, Spray pyrolysis, Yttrium, Antimicrobial activity.*

1. Introduction

In aquaculture, there is a several bacterial diseases lead to increased use of antibiotics; still antibiotics have several disadvantages in aquaculture. Antibiotics are added to foods that settle in the water, so that they can build up in the fish. Increase in global fish consumption have resulted in greater development and intensification of aquaculture worldwide (Goldburg and Naylor et al., 2005; Cabello et al., 2008) which have led to a massive use of antibiotics for promoting growth and prophylaxis, especially in intensive aquaculture (Cabello et al., 2008). Since last decade, the problem of antibiotic resistance has become a major concern in human and veterinary medicine (Menanteau Ledoubl et. al., 2015; Sørum et al., 2008). The unregulated and excessive use of antibiotics leads to the emergence of antibiotic resistance in fish pathogenic bacteria. Multi-drug resistant bacteria have been isolated from fish, sediment, and water of farms (Austin & Austin et al., 2016; Shaalan et al., 2016). Sørum, 2008 has reported the emergence of antibiotic resistant strains of *Aeromonas hydrophila, Aeromonas salmonicida,* and *Yersinia ruckeri* in fish farms (Sørum et al., 2008). Researchers conducted a study on the use of antimicrobial in fish farms in 25 countries. They found that tetracycline was the most widely used antibiotic in fish farms. Antibiotic resistance has been seen in Aeromonas salmonicida and Photobacterium damselae. The broad-spectrum antibiotics tetracycline, streptomycin, and erythromycin are found from the species of Aeromonas hydrophila grown from tilapia. They suggested that the fish-resistant bacteria could transmit the infection to humans and that the presence of these fish in fishponds became a significant public health issue (Shaalan et al., 2016).

As genetic elements can be shared between aquatic and terrestrial bacteria, human and animal pathogens can acquire such antibiotic-resistance genes from fish pathogens which cause public health issues recently (Swain et al., 2014; Luis et al., 2019). Thus, there is an urgent need to establish some novel strategies to combat antibiotic-resistance development and disease outbreaks in aquaculture without affecting the aquatic ecosystem. Different nanomaterials, such as TiO_2, MgO, Ag_2O and ZnO, have been studied as potential antibacterial agents (Sawai et al., 2003; Armelao et al., 2007; Hu et al., 2012).

Interestingly, Zinc Oxide nanoparticles (ZnO NPs) are emerging as a most promising metal based nanodrugs due to their biocompatibility, selectivity, and high potency (Bisht & Rayamajhi, 2016; Elshama et al., 2018; Jin & Jin 2019). ZnO NPs exhibit potent antimicrobial activities (Shaalan, et al., 2013; Swain et al., 2014; Gunalana et al., 2012), which are suspected of arising through complex mechanisms of action that include release of Zn^{2+} ions, production of ROS and interference with bacterial replication by inhibition of cellular processes like glycolysis, acid tolerance and trans membrane proton translocation (Seil & Webster et al., 2012; Sirelkhatim et al., 2015). There are recent reports on the application of ZnO-NPs in aquaculture as an alternative of conventional zinc sources as feed additive to promote growth (Faiz et al., 2015; Wang et al., 2017; Onuegbu et al., 2018) and immunity (Anjugam et al., 2018; Awad et al., 2019).

Doped nanomaterials, especially rare earth doped-ZnO nanoparticles, have shown interesting and improved physical and chemical properties. La, Ce, Dy, and Gd-doped ZnO nanoparticles have been used as antimicrobial agents against *Pseudomonas aeruginosa*, *Staphylococcus aureus* and *Salmonella paratyphi-B*, among others (Pratap et al., 2018; Kayani et al., 2019; Anitha & Muthukumaran, 2020). To the best of our knowledge, investigation on the effect of Yttrium-doped ZnO nanomaterials on antibiotic resistant fish pathogens is lacking in the literature. Therefore, in this study, we have investigated the antibacterial activity of yttrium (2, 4, 6 at. %) doped ZnO thin films against fish pathogens viz., *Aeromonas hydrophila, Lactococcus garvieae, Salmonella enterica and Streptococcus agalactiae.*

Generally, the high quality metal oxide thin films are fabricated by different bottom up approaches such as sol-gel fabrication (Co-precipitation), Hydrothermal, Chemical Bath Deposition (CBD), Successive Layer Adsorption and Reaction (SILAR), DC Magnetron sputtering, Pulsed Laser Deposition(PLD), electro deposition, spin coating, Spray Pyrolysis, etc., (Vasanthi et al., 2014). Compared with other synthesis techniques, Spray pyrolysis is the most effective alternative method for producing metal oxide thin films at higher temperatures. The researchers frequently use this deposition method to create both doped and undoped metal oxide semiconducting thin films due to its affordability (Ravichandran et al., 2014). This method is appropriate for easily depositing thin films because it involves simultaneous chemical and thermal reactions with a very high growth rate at higher substrate temperatures. It is noteworthy to mention that in the current work, the pure ZnO and yttrium doped ZnO:Y films are deposited on a glass substrate at constant substrate temperature and ambient pressure using a straightforward, vacuum-free, and most importantly low cost, constructed in our laboratory itself, spray pyrolysis instrument. The experimental demonstration of this simplified spray pyrolysis set up is shown in Fig. 1.

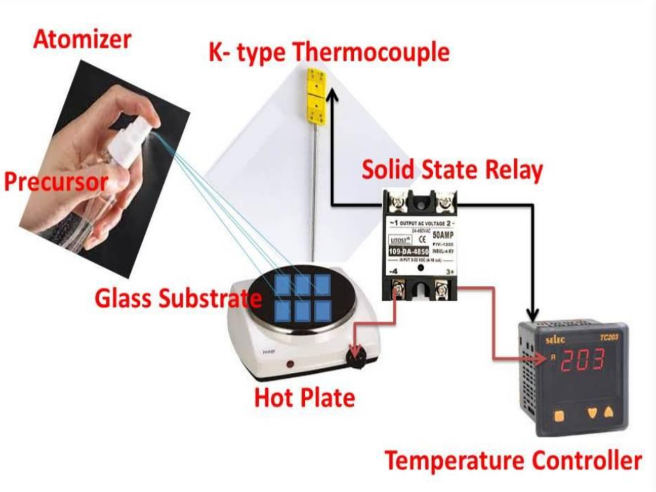

Fig. 1 Experimental arrangement of Simplified Spray Pyrolysis Setup

2. Materials and Methods

2.1 Preparation of ZnO:Y thin films

For the film deposition, high purity chemical reagents (Sigma Aldrich 99.9%) were used. Zinc acetate dihydrate ($Zn(COOCH_3)_2.2H_2O$) was taken as the starting material. The Yttrium nitrate hexahydrate ($Y(NO_3)_3.6H_2O$) was used as dopant precursor and its concentration was varied as 2, 4 and 6 at. % in the starting solution. The distilled water was used as the solvent. Initially, the glass substrate was immersed in concentrated hydrochloric acid for etching the substrate surface for a few seconds and wiped with distilled water and the substrate was immerged in acetone for a few seconds to remove visible contamination, surface oxides and precipitation. Finally, the substrate was cleaned by the cotton. The substrates have been dried in the air and been placed on the heating plate for film deposition.

The pure ZnO thin films were deposited from a 0.1 M precursor solution containing zinc acetate dihydrate dissolved in 50 ml of distilled water and continuously stirred for a few minutes. A few drops of the complexing agent acetic acid were added to the solution to obtain a transparent precursor solution. For ZnO:Y films, the precursor solution containing zinc acetate dihydrate and various atomic percentages of yttrium nitrate hexahydrate (2, 4, and 6 at. %) was added to the mixture. The prepared precursor solution was taken in spray bottle at a flow rate of 5 ml/min. The well cleaned substrates are placed on the heating plate to achieve the constant substrate temperature of 350 °C maintained by the K-type thermocouple, and a distance of 30 cm is maintained between the substrate and the spray nozzle. The prepared precursor solution was sprayed on the glass substrate at ambient pressure, where thermal decomposition takes place to form the pure ZnO and ZnO:Y thin film layers on the substrate. All the deposition parameters were kept constant for all the films. Then, the deposited films were subjected to different characterization techniques to study their physical characteristics.

2.2. Characterization employed

The structural properties of the prepared films were investigated by X-ray diffractometer (PANalytical-PW 340/60 X'pert PRO) with Cu-K_α radiation of wavelength λ=1.540 Å. The elemental composition of the deposited films was studied using Perkin Elmer RX-I FTIR spectrophotometer. The optical properties of the films were studied with the help of UV-Visible-NIR spectrophotometer (UV-1700 Shimadzu) and Spectrofluorometer (JobinYvon-FLUROLOG-FL3-11). The surface morphology of the films was studied using scanning electron microscope (SEM–HITACHIS-3000 H).

2.3. Screening of Antibacterial characteristics

The *in-vitro* antibacterial analysis was done against the fish pathogenic bacteria *viz*., *Aeromonas hydrophila*, *Lactococcus garvieae*, *Salmonella enterica* and *Streptococcus agalactiae*. Agar well diffusion method with slight modification was carried out for this assay. Brain heart infusion (BHI) broth was used for culturing the pathogens. Overnight cultures with the cell density 10^{-4}cfu/ml were used for the experiment. The sterilized MHA (25ml /plate) were incorporated on to petri dishes and left for a while till it gets solidified. Fresh overnight cultures of four pathogens were then spread plated using sterile cotton swabs. As our synthesized nanoparticles are coated on the glass slides, the portion of coated glass slides was cut into small pieces and placed on the petri-plates in inverted position so as to bring the nanoparticles in direct contact with the pathogens. The undoped and yttrium (2, 4, 6 at. %) doped ZnO films were then allocated into their respective places (Logeswari et al., 2013). A standard antibiotic disc was manually kept over petridish at center. Incubation was carried out at 37 °C overnight and seen next day as presence or absence of a zone of Inhibition (Gokulakrishnan et al., 2012).

3. Results and Discussion

3.1. XRD Analysis

Fig. 2 shows the X-ray diffractograms of the undoped ZnO and different at. % of Yttrium doped ZnO thin films. In all the samples, the XRD patterns show the phase homogeneity and the same prominent peaks indicating that the crystal structure of the all deposited films show hexagonal (wurtzite) phase with highly preferential orientation along (002). The relative intensities of the peaks, observed in the XRD patterns are to be in a good agreement with those indicated by the Joint Committee on Powder Diffraction Standards (JCPDS) for the wurtzite structure of ZnO (card No. 36–1451). In all of the examined films, there were no extra peaks of Y, indicating the segregated Y-rich phases. This indicates that the doping material (Y^{3+}) is well assimilated into the host lattice of ZnO through the samples. These results are good agreement with previous results reported by Miller et al., and Lim et al., 2011.

The high crystal quality of Y doped ZnO films can be deduced by the lower ionization energy of Y. In other words, the Y dopants having low ionization energy that release the difference between the surface free energy of Si and the c-axis preference energy of ZnO. As a result, crystalline Y doped ZnO films could be easily grown on the Si substrate even without any catalyst (Prasad Rao et al., 2009).

The intensity of the (002) peak is maximum for pure ZnO film, showing that the film have a good crystalline nature even before doping. A decrease in the intensity of (002) reflection is noticed after increasing the doping concentration beyond 4 at. % suggesting a loss of crystallinity, because of the isolation of Y at grain boundaries for high doping contents. The position of the (002) peak intensity is gradually shifted at the lower scattering angle (2θ) side while increasing doping concentration up to 4 at. %. This trend may be attributed to the a substitution of Zn^{2+} (0.74 Å) by Y^{3+} ions (0.92 Å). The similar trend is observed for metal oxide films while doping Y for Srinivasalu et al., 2017). The interplanar spacing d_{hkl} values of undoped ZnO and Y doped ZnO thin films were calculated using the Bragg's equation (Debye & Scherer et al., 1916). The crystallite size of the samples was determined based on the broadening of the preferential orientation (002) using the Debye-Scherer's formula (Scherer & Göttinger Nachrichten, 1918),

$$D = \frac{k\lambda}{\beta\cos\theta} \quad (1)$$

Where k represents the shape factor (0.9), β is the full width at half maximum in radian of (002) orientation, λ is the X-ray wavelength (0.154 nm) and θ is the Bragg's angle of the X-ray diffraction peak. The micro strain and the dislocation density were also determined for each film by using the tangent formula (Mehedi Hassan et al., 2014),

$$\beta_{hkl}\cos\theta = \frac{k\lambda}{D} + 4\varepsilon\sin\theta \quad (2)$$

and

$$\text{Dislocation density } (\delta) = \frac{1}{D^2} \quad (3)$$

The calculated values of average crystallite size (D), lattice constant (c), strain (ξ) and dislocation density (δ) values for the different samples are listed in Table 1. The average crystallite size is fall in the range between 4 to15 nm. From the results, it can be observed that doping of Yttrium at a certain level (4 at. %) improves the structural quality of sprayed pure ZnO thin films, decrease in the crystallite size (D) which in turn decrease in the micro-strain. This result indicates that the home made simplified spray pyrolysis could be capable of producing high crystalline quality thin films.

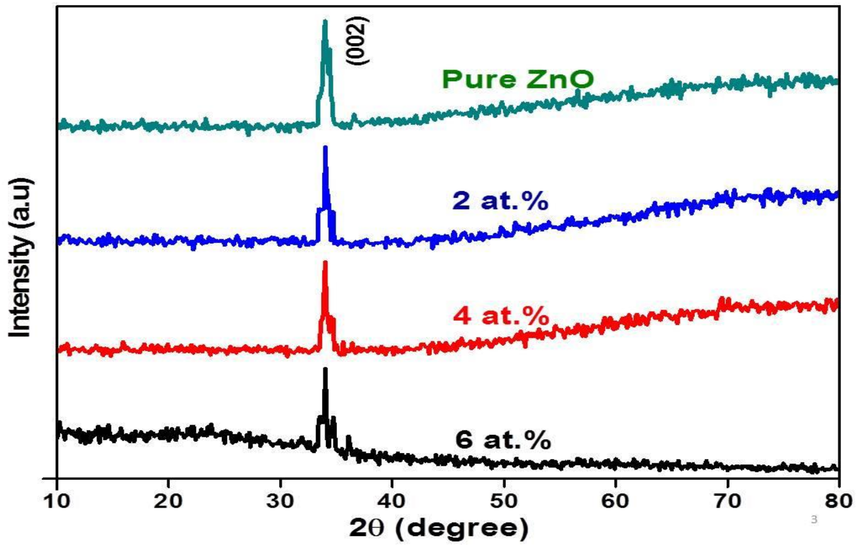

Fig. 2 X-ray diffractograms of undoped and Y doped ZnO thin films

Table 1: Structural parameters of undoped and ZnO:Y thin films

Sample	Average Crystallite Size (D) (nm)	Lattice Constant (c) [Å]	Strain (ε)	Dislocation Density (δ) (lines/m^2)
ZnO	14.47	5.218	0.4504	4.775x10^{16}
ZnO:Y (2 at. %)	9.03	5.210	0.7255	1.226 x10^{16}
ZnO:Y (4 at. %)	4.04	5.188	0.1262	6.128 x10^{16}
ZnO:Y (6 at. %)	5.16	5.192	0.2242	3.755 x10^{16}

3.2. FTIR analysis

The FTIR spectra were recorded in the range of 400-4000 cm^{-1} for deposited films and the peaks confirm the various chemical bonds that are present in thin films and are shown in Fig. 3. The spectra clearly show that the vibrational peaks range from 400 to 500 cm^{-1} which confirms the presence of ZnO stretching vibrations as reported in the literature (Anandan S et al., 2013). The narrow small peak at 846 cm^{-1} corresponding to the C-N stretching peak. The vibrational bonds within 1000 cm^{-1} are may be due to inorganic elements present in the samples. C=O vibration is observed at 1509 and 1601 cm^{-1} (Thirumoorthi et al., 2015). The bands at 1513 and 1417 cm^{-1} are assigned to the vibration of the carboxylic group and CO_2 observed in air, respectively, (Shek Dhavud et al., 2020). Moreover, the C-O bond is located at a vibrating frequency of 1384 cm^{-1}. A small band around 1604 cm^{-1} is assigned to bending H–O–H vibration of the water molecules adsorbed on the surface of ZnO. The characteristic IR peaks below 633 cm^{-1} is ascribed to presence of ZnO–Y bond (Chen K et al., 2009).The Y-O stretching characteristic peak is observed at 505–562 cm^{-1}(Liu J, 2011; Raja K et al., 2014) which strongly confirms the incorporation of Y^{3+} ions on Zn^{2+} sites of ZnO matrix. The band occurring near 727 cm^{-1} is attributed to the vibrations of Y-ZnO local bond (Repelin et al., 1995). The O-H deformation vibration is observed at 1667 cm^{-1}. We found that the hydroxyl groups of N-O, C-H, =C-H and C-N vibrations shows that alkane and alkene groups present in the deposited films (Sato et al., 1988; Muneer et al., 2013; Mitra et al., 2013).

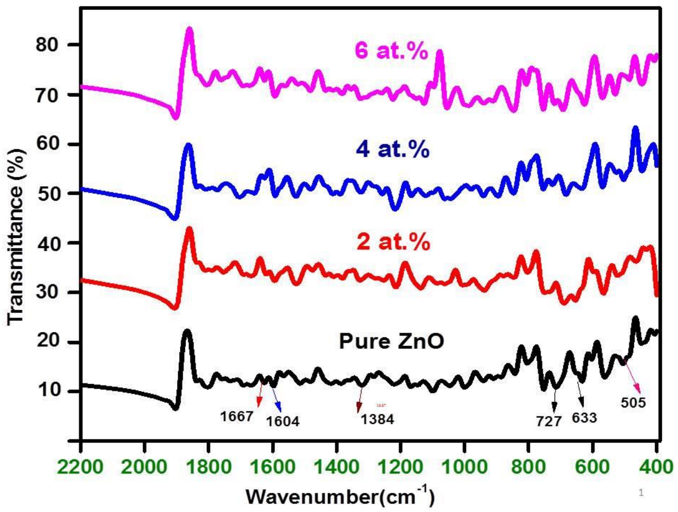

Fig. 3 FTIR Spectra of undoped and Y doped ZnO thin films

3.3. Optical Study

The transmittance spectra of undoped and Yttrium doped ZnO thin films are shown in Fig. 4. From this figure, it can be observed that all the deposited films are having good transparency in visible and near infrared region. The undoped ZnO and ZnO:Y films show the average transmittance of 75 % in 600 to 1200 nm wavelength region. The absence of interference fringes in the spectra indicates that there are no reflections at the air/film and film/substrate interface (Byeongyum et al., 2006). Most of the literature showed that different dopants exhibits different optical transmittance due to optical losses in deposited film. Generally, the good crystalline nature of the deposited films is an identification of the sharp fall in the transmission near the fundamental absorption edge owing to the reduction in loss of incident electromagnetic radiation (Salakan et al., 2013). Hence, in the present study the observed sharp fall in the transmission spectra strongly support our XRD findings.

In the visible region, undoped ZnO exhibits high optical transparency, confirming the homogeneity and smoothness of the produced sample in the absence of yttrium. The transmittance in the visible range drops (increased absorption) when the yttrium is doped, and the red shift is observed for exciton peak (365 nm). This behavior is remarkable for the sample doped with 4 at. % of yttrium (inset of Fig. 4). This outcome is comparable to the findings that increased absorbance causes visible-light photo activity (Gotkas et al., 2013). These results are in good agreement with the reports of Cheng et.al (Shan et al., 2005). As with the Y-doping concentration, 4 at.% demonstrated greater NIR transmittance than the other doped films, which is likely due to the elimination of light scattering with decreasing carrier concentration. It is crucial to note here that a metal oxide's with increased visible light absorption results an enhanced antibacterial action. This finding is corroborated by Cheng et al.'s study on the effect of oxide-based NPs on fish infections that have visible light activated bactericidal activity (Numan Salah et al., 2013).

The optical energy band gap (E_g) of films can be determined by studying variation of optical absorption coefficient with wavelength of incident photons by the material (Bakin et al., 2010) using Tauc's relation,

$$\alpha h\nu = B(h\nu - E_g)^n \quad (4)$$

Here, h is plank constant, α is the absorption coefficient, E_g is optical band gap energy and B is proportionality constant. The figure 5 shows the different energy band gap (E_g) values (Tauc's Plot) of the deposited films. The calculated values are found to be 3.11 eV, 3.05 eV, 3.02 eV and 3.01 eV for pure and 2 at. %, 4 at. % and 6 at. % of yttrium doped ZnO films, respectively.

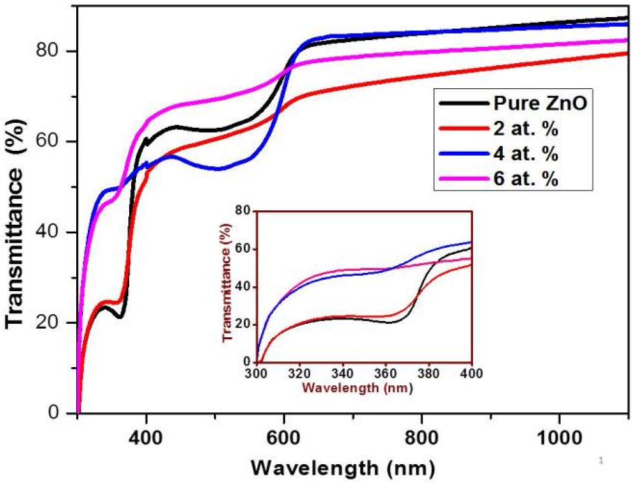

Fig. 4 Transmittance spectra of undoped and Y doped ZnO thin films

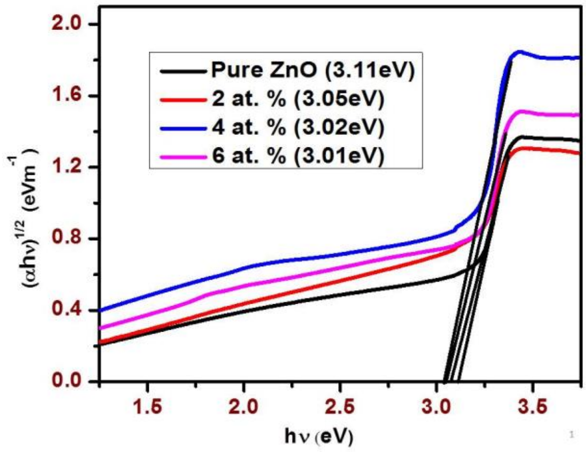

Fig. 5 Tauc's plots of undoped and Y doped ZnO thin films

3.4 Photoluminescence Study:

Fig. 6 Shows the room temperature PL spectra of ZnO:Y thin films with respect to Y concentration (0, 2, 4 and 6 at. %). From this figure, we found that the Y concentration affected the PL emission. All samples showed two major ultraviolet (UV) emission peaks: i.e. an intense peak located at 330 nm and a broad deep level emission peak in the region of 370 - 400 nm. We observed increasing UV emission by the incorporation of Y concentration (2 at. %) due to the reduced defects, such as oxygen vacancies and zinc vacancies (Ahmad Umar et al., 2015). The replacement of higher ionic radii element (Y^{3+}) (0.1011 nm) with smaller ionic radii element (Zn^{2+}) can expand the local volume of the lattice, which may reduce the defects (Kaur et al., 2016). However further increase in Y (4 and 6 at. %) doping causes the phase segregation and also results, the broad deep level emission in the region (370 - 400 nm). This is related with the free exciton recombination of ZnO. At higher concentration of Y, it is unable to replace Zn but occupies some interstitial position in the host lattice resulting in the phase segregation (Kumar et al., 2015).

Oxygen vacancies are usually reported to be responsible for this emission band. 2 and 6 at. % of Y: ZnO shows less emission in UV region, but 4 at. % of Y doped ZnO shows more emission comparing with pure and other doped materials due to enhanced incorporation of Yttrium suppresses the deep level defects and reinforces the UV emission. It is valuable to note that this band is most frequently reported band for ZnO material (Suvith et al., 2014).

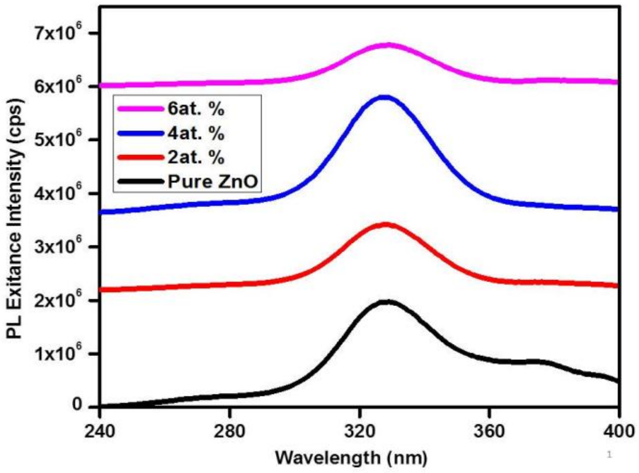

Fig. 6 PL Emission spectra of undoped and Y doped ZnO thin films

3.5. Surface Morphological Study

Fig. 7 shows the SEM images of the ZnO thin films coated with different Y doping levels: 0, 2, 4 and 6 at. %. It can be noticed from the figure that the pure ZnO thin film has a spherical-like shaped grains with good uniformity. On the other hand, pinholes and groupings of particles were also seen. 2 at. % of yttrium substituted ZnO film exhibits cauliflower-like structure and demonstrates substantial morphological alterations. From this observed abrupt change in morphology, it is highly suggested that yttrium was incorporated into the ZnO lattice (Dghoughi et al., 2010). In comparison to the morphology obtained for a 2 at. % of yttrium doped ZnO thin film, the film exhibits a tetra pod chain like structure with an enhanced surface to volume ratio at 4 at.% of yttrium doping. That is on the substrate surface, several ongoing hollow tube growths are observed. As reported by Xu et al. (Yaoming Li et al., 2010) this hollow design could be useful for capturing biomolecules and microbes. The 4 at. % of Yttrium doped ZnO sample is therefore thought to have improved antibacterial effectiveness. The 6 at. % of Yttrium doped ZnO sample may be seen to have some broken tetra pod chains and background grains that are somewhat spherical. This morphology-changing behavior may be caused by the interstitial entry of yttrium ions into the ZnO lattice, which leads to the development of tension between zinc and yttrium ions (Shinde et al., 2006; Yu Q et al., 2007).

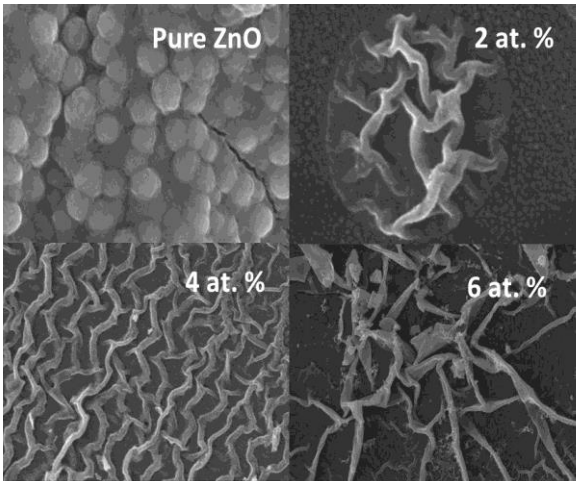

Fig. 7 SEM images of undoped and Y doped ZnO thin films

3.6. Antibacterial study:

Fig. 8 shows zone of inhibitions of pure and yttrium doped ZnO thin films against, antibiotic resistant fish bacteria *viz*., *Aeromonas hydrophila, Salmonella enterica, Lactococcus garvieae* and *Streptococcus agalactiae.* All the deposited films (0, 2, 4, 6 at. % of Y) was identified as having potent antibacterial activity against the examined pathogens. The diameter of inhibition zones around each well is measured in millimeters and represented as bar diagram (Fig. 9). From this figure, it can also be observed that the prepared samples exhibit more sensitive antibacterial nature compared with standard samples.

The current results indicate that the degree of zone of inhibition (with mean ± SD values) was more against gram negative bacterial strains *Aeromonas hydrophila, Salmonella enterica* when compared to the gram positive bacteria Lactococcus garvieae and *Streptococcus agalactiae..* Similar results were published by **(**Maddahi et al. 2012), for gram negative and gram positive bacterial strains. The difference in structural organization between gram positive and gram negative bacterial cell wall is a well-known fact. Due to the presence of thicker peptidoglycan layer in gram positive bacteria, they are less prone to nanotoxicity of ZnO:Y nanoparticles when compared to gram negative bacteria. This might be the reason for the obtained results that indicates high degree of inhibition zone in the case of gram negative bacteria when compared to gram positive Bacteria.

ZnO is a highly effective metal oxide nanoparticle that can readily control the bacteria growth (Raghupathi et al., 2011; Gunalan et al., 2012; Salini et al., 2021). According to the antibacterial mechanism of ZnO, the ZnO matrix may easily release the Zn^{2+} ions and this can directly contact with bacterial cells. Zn^{2+} nanoparticles contact with inside and outside of the cell walls and it causes the damage and destruction of cell walls and membrane. The cell wall is mainly composed of peptidoglycan, which has a negative charge due to the presence of carboxyl, phosphate, and amino groups. The positive charge of Zn nanoparticles confers electrostatic attraction between Zn and negatively charged cell membrane of the microorganisms. Hence, stronger attractive force can be achieved by altering the surface charge of Zn NPs to improve the antibacterial effects. Zn NPs can penetrate inside microbial cell, and released Zn^{2+} can interact with cellular structures and biomolecules such as enzymes, lipids, proteins and DNA. Zn NPs can sustainably release Zn^{2+} in and out of bacteria, and Zn ions can interact with proteins and enzymes. The Zn nanoparticles can bind to the protein easily present in the cell membrane, which are involved in trans-membrane ATP generation. The cytoplasmic injury occurred in different degrees inside the cell causes the cell to lose its cell shape. The increased reactive oxygen species (ROS) lead to an apoptosis-like response, lipid peroxidation, and DNA damage (Qing et al., 2018). Even though the aforesaid antibacterial mechanism is believed to be true, the exact antibacterial mechanism of ZnO nanoparticles is still unknown.

The reason for enhanced efficacy of Y doped ZnO thin films is that the dopant yttrium is containing ability to suppress the growth of both gram- positive and gram- negative bacteria. Yttrium increases the inhibitory effect and production of reactive oxygen species and aggregation of Y: ZnO nanoparticles in the membrane and plasma of the cell to produce excellent anti-bacterial activity (Tam et al., 2008; Sharma et al., 2010).

The range of inhibition depends on the concentration of nanoparticles. In YZO thin films up to Y concentration of 4 at. % is related to the substitution of Y^{3+} ions at Zn^{2+} cation sites, and as a consequence increase in the liberation of Zn^{2+} and Y^{3+}ions from the film was anticipated which support the observed enhancement in the antibacterial efficiency of the synthesized samples. Maria magdalane et al.,;Kaviyarasu K et al., reported that Y^{3+} ions discharged from Y:ZnO act as positive charge reacts with the cell having negative charge leading to the decay of proteins.

Further increasing the Y concentration beyond 4 at. % leads to the higher incorporation of interstitial Y atoms giving rise to segregation of grain boundaries. It is well known that grain boundary segregation of impurities in nanomaterials also affects other materials properties controlled by interfaces (Manoharan et al., 2015) Grain boundary segregation can also have an important effect on the reduction of grain boundary mobility (Thongsuriwong et al., 2012) and, consequently, on the recrystallization temperature and stabilization of nanocrystalline structures (Singh et al., 2009; Maddahi et al., 2014). Hence, in the present study YZO films with higher concentration (6 at. %) is found to have decreased crystallinity which in turn leads to decreased antibacterial efficacy. The decreased crystallinity of 6 at. % of YZO films can be strongly evidenced by XRD and SEM studies. Thus, the antibacterial activity of deposited films against pathogenic bacteria depends on its size, surface area and concentration of dopant ions (Mote et al., 2014). Thus, an appropriate concentration of Y in ZnO thin films improves the crystallinity, which allows us to tailor the physical, optical, and antibacterial properties to make better and more stable nanomaterials (Azam et al., 2012).

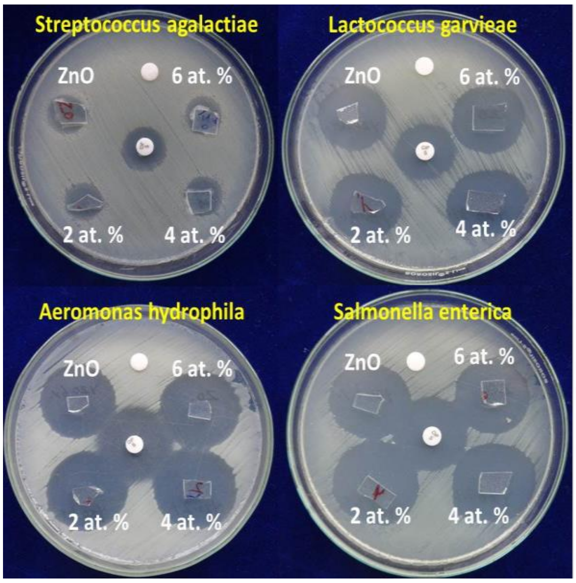

Fig. 8 Zone of inhibitions of pure ZnO and Y doped ZnO

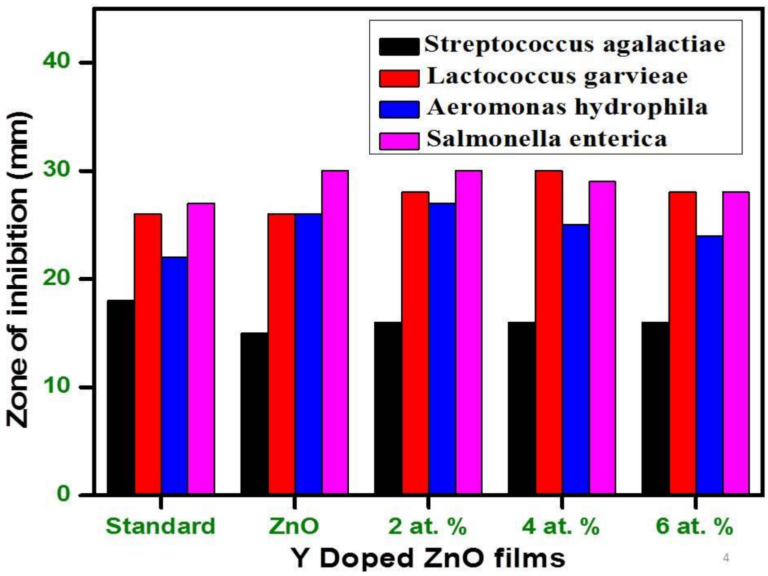

Fig. 9 Bar diagram- antibacterial efficacy of Deposited Films

4. Conclusion

This paper attempts to examine the advancements of synthesized metal nanoparticles as antibacterial agents, focusing on their toxicity and antibacterial activity based on the structure, dimensions and size of nanoparticals. To the best of our knowledge, this study on inhibitory effects of yttrium doped zinc oxide thin films prepared using simplified spray technique towards the fish pathogens *Aeromonas hydrophila*, *Salmonella enterica,* Lactococcus garvieae and *Streptococcus agalactiae.* Based on the results, it can be concluded that gram negative organisms have shown greater sensitivity to the final product than gram positive organisms to metal oxide nanoparticles. The concentration of the nanoparticle plays a significant role in the resolution of antibacterial activity. The 4 at.% of yttrium doped ZnO sample have improved antibacterial effectiveness among all the prepared samples. The surface area of the metal oxide nanoparticles that comes in contact with bacterial cells is directly proportional to the extent of antimicrobial activity recommended by the particle. The obtained results make clear the significance of using yttrium doped ZnO thin films as a novel, therapeutic approach to reduce fish bacterial infections, but extensive *in-vivo* testing is required to determine the product's therapeutic value. It is hoped that the present results of the current review article will take a step towards the need to use as much as possible and, of course, cautiously in the use of nanoparticles in the aquaculture industry.

Funding: The authors received no specific funding for this work

Compliance with ethical standards

Conflict of interest: The authors declare that they have no conflict of interest.

References

[1] A review on zinc sulphide nanoparticles: From synthesis, properties to applications. (2016). Journal of Bioelectronics and Nanotechnology, 1(1). https://doi.org/10.13188/2475-224X.1000006.

[2] Anandan, S., & Muthukumaran, S. (2013). Influence of Yttrium on optical, structural and photoluminescence properties of ZnO nanopowders by sol–gel method. Optical Materials, 35(12), 2241–2249. https://doi.org/10.1016/j.optmat.2013.06.009.

[3] Anitha, S., & Muthukumaran, S. (2020). Structural, optical and antibacterial investigation of La, Cu dual doped ZnO nanoparticles prepared by co-precipitation method. Materials Science and Engineering: C, 108, 110387. https://doi.org/10.1016/j.msec.2019.110387.

[4] Anjugam, M., Vaseeharan, B., Iswarya, A., Gobi, N., Divya, M., Thangaraj, M. P., & Elumalai, P. (2018). Effect of β-1, 3 glucan binding protein based zinc oxide nanoparticles supplemented diet on immune response and disease resistance in Oreochromis mossambicus against Aeromonas hydrophila. Fish & Shellfish Immunology, 76, 247–259. https://doi.org/10.1016/j.fsi.2018.03.012.

[5] Armelao, L., Barreca, D., Bottaro, G., Gasparotto, A., Maccato, C., Maragno, C., Tondello, E., Štangar, U. L., Bergant, M., & Mahne, D. (2007). Photocatalytic and antibacterial activity of TiO 2 and Au/TiO 2 nanosystems. Nanotechnology, 18(37), 375709. https://doi.org/10.1088/0957-4484/18/37/375709.

[6] Austin, B., & Austin, D. A. (2016). Bacterial fish pathogens. Springer International Publishing. https://doi.org/10.1007/978-3-319-32674-0.

[7] Awad, A., Zaglool, A. W., Ahmed, S. A. A., & Khalil, S. R. (2019). Transcriptomic profile change, immunological response and disease resistance of Oreochromis niloticus fed with conventional and Nano-Zinc oxide dietary supplements. Fish & Shellfish Immunology, 93, 336–343. https://doi.org/10.1016/j.fsi.2019.07.067.

[8] Azam, A., Ahmed, Oves, Khan, Habib, & Memic, A. (2012). Antimicrobial activity of metal oxide nanoparticles against Gram-positive and Gram-negative bacteria: A comparative study. International Journal of Nanomedicine, 6003. https://doi.org/10.2147/IJN.S35347.

[9] Ba-Abbad, M. M., Kadhum, A. A. H., Bakar Mohamad, A., Takriff, M. S., & Sopian, K. (2013). The effect of process parameters on the size of ZnO nanoparticles synthesized via the sol–gel technique. Journal of Alloys and Compounds, 550, 63–70. https://doi.org/10.1016/j.jallcom.2012.09.076.

[10] Bakin, A., Behrends, A., Waag, A., Lugauer, H.-J., Laubsch, A., & Streubel, K. (2010). Zno-gan hybrid heterostructures as potential cost-efficient led technology. Proceedings of the IEEE, 98(7), 1281–1287. https://doi.org/10.1109/JPROC.2009.2037444.

[11] Bakin, A., El-Shaer, A., Mofor, A. C., Al-Suleiman, M., Schlenker, E., & Waag, A. (2007). ZnMgO-ZnO quantum wells embedded in ZnO nanopillars: Towards realisation of nano-LEDs. Physica Status Solidi c, 4(1), 158–161. https://doi.org/10.1002/pssc.200673557.

[12] Cabello, F. C. (2006). Heavy use of prophylactic antibiotics in aquaculture: A growing problem for human and animal health and for the environment. Environmental Microbiology, 8(7), 1137–1144. https://doi.org/10.1111/j.1462-2920.2006.01054.x.

[13] Chen, K. J., Hung, F. Y., Chang, S. J., & Young, S. J. (2009). Optoelectronic characteristics of UV photodetector based on ZnO nanowire thin films. Journal of Alloys and Compounds, 479(1–2), 674–677. https://doi.org/10.1016/j.jallcom.2009.01.026.
[14] Chris, U. O., Singh, N. B., & Agarwal, A. (2018). Nanoparticles as feed supplement on Growth behaviour of Cultured Catfish (Clarias gariepinus) fingerlings. Materials Today: Proceedings, 5(3), 9076–9081. https://doi.org/10.1016/j.matpr.2017.10.023.
[16] Dghoughi, L., Ouachtari, F., Addou, M., Elidrissi, B., Erguig, H., Rmili, A., & Bouaoud, A. (2010). The effect of Al-doping on the structural, optical, electrical and cathodoluminescence properties of ZnO thin films prepared by spray pyrolysis. Physica B: Condensed Matter, 405(9), 2277–2282. https://doi.org/10.1016/j.physb.2010.02.025.
[17] Djearamane, S., Lim, Y. M., Wong, L. S., & Lee, P. F. (2018). Cytotoxic effects of zinc oxide nanoparticles on cyanobacterium Spirulina (Arthrospira) platensis. PeerJ, 6, e4682. https://doi.org/10.7717/peerj.4682.
[18] Elshama, S. S., Abdallah, M. E., & Abdel-Karim, R. I. (2018). Zinc oxide nanoparticles: Therapeutic benefits and toxicological hazards. The Open Nanomedicine Journal, 5(1), 16–22. https://doi.org/10.2174/1875933501805010016.
[19] Faiz, H., Zuberi, A., Nazir, S., Rauf, M., & Younus, N. (2015). Zinc oxide, zinc sulfate and zinc oxide nanoparticles as source of dietary zinc: Comparative effects on growth and hematological indices of juvenile grass carp(Ctenopharyngodon idella). International Journal of Agriculture and Biology, 17(3), 568–574. https://doi.org/10.17957/IJAB/17.3.14.446
[20] Goktas, A., Mutlu, I. H., & Yamada, Y. (2013). Influence of Fe-doping on the structural, optical, and magnetic properties of ZnO thin films prepared by sol–gel method. Superlattices and Microstructures, 57, 139–149. https://doi.org/10.1016/j.spmi.2013.02.010.
[21] Goldburg, R., & Naylor, R. (2005). Future seascapes, fishing, and fish farming. Frontiers in Ecology and the Environment, 3(1), 21–28. https://doi.org/10.1890/1540-9295(2005)003[0021:FSFAFF]2.0.CO;2.
[22] Gunalan, S., Sivaraj, R., & Rajendran, V. (2012). Green synthesized ZnO nanoparticles against bacterial and fungal pathogens. Progress in Natural Science: Materials International, 22(6), 693–700. https://doi.org/10.1016/j.pnsc.2012.11.015.
[23] Hassan, M. M., Khan, W., Azam, A., & Naqvi, A. H. (2014). Effect of size reduction on structural and optical properties of ZnO matrix due to successive doping of Fe ions. Journal of Luminescence, 145, 160–166. https://doi.org/10.1016/j.jlumin.2013.06.024.

[24] Hu, H., Zhang, W., Qiao, Y., Jiang, X., Liu, X., & Ding, C. (2012). Antibacterial activity and increased bone marrow stem cell functions of Zn-incorporated TiO2 coatings on titanium. Acta Biomaterialia, 8(2), 904–915. https://doi.org/10.1016/j.actbio.2011.09.031.
[25] Jin, S.-E., & Jin, H.-E. (2019). Synthesis, characterization, and three-dimensional structure generation of zinc oxide-based nanomedicine for biomedical applications. Pharmaceutics, 11(11), 575. https://doi.org/10.3390/pharmaceutics11110575.
[26] Jin, S.-E., & Jin, H.-E. (2021). Antimicrobial activity of zinc oxide nano/microparticles and their combinations against pathogenic microorganisms for biomedical applications: From physicochemical characteristics to pharmacological aspects. Nanomaterials, 11(2), 263. https://doi.org/10.3390/nano11020263.

[27] Kaviyarasu, K., Maria Magdalane, C., Kanimozhi, K., Kennedy, J., Siddhardha, B., Subba Reddy, E., Rotte, N. K., Sharma, C. S., Thema, F. T., Letsholathebe, D., Mola, G. T., & Maaza, M. (2017). Elucidation of photocatalysis, photoluminescence and antibacterial studies of ZnO thin films by spin coating method. Journal of Photochemistry and Photobiology B: Biology, 173, 466–475. https://doi.org/10.1016/j.jphotobiol.2017.06.026.

[28] Kayani, Z. N., Sahar, S., Riaz, S., & Naseem, S. (2019). Tuning of optical and antibacterial characteristics of ZnO thin films: Role of Ce content. Ceramics International, 45(3), 3930–3939. https://doi.org/10.1016/j.ceramint.2018.11.066.

[29] Kompany, A., Madahi, P., Shahtahmasbi, N., & Mashreghi, M. (2012). Synthesis, characterization and antibacterial property of ZnO:Mg nanoparticles. 555–558. https://doi.org/10.1063/1.4757533.

[30] Li, Y., Xu, L., Li, X., Shen, X., & Wang, A. (2010). Effect of aging time of ZnO sol on the structural and optical properties of ZnO thin films prepared by sol–gel method. Applied Surface Science, 256(14), 4543–4547. https://doi.org/10.1016/j.apsusc.2010.02.044.

[31] Lie, Ø. (2008). Improving farmed fish quality and safety. CRC press Woodhead publ.

[32] Lim, S. J., Kwon S. J., Kim, H., (2008). ZnO thin films prepared by atomic layer deposition and RF sputtering as an active layer for thin film transistor. Thin Solid Films, 516(7), 1523–1528. https://doi.org/10.1016/j.tsf.2007.03.144.

[33] Liu, J., Zhao, C., Li, Z., Chen, J., Zhou, H., Gu, S., Zeng, Y., Li, Y., & Huang, Y. (2011). Low-temperature solid-state synthesis and optical properties of CdS–ZnS and ZnS–CdS alloy nanoparticles. Journal of Alloys and Compounds, 509(39), https://doi.org/10.1016/j.jallcom.2011.07.0029428–9433.

[34] Luis, A. I. S., Campos, E. V. R., De Oliveira, J. L., & Fraceto, L. F. (2019). Trends in aquaculture sciences: From now to use of nanotechnology for disease control. Reviews in Aquaculture, 11(1), 119–132. https://doi.org/10.1111/raq.12229.

[35] M., P. K., G.A, S. J., G., T., A., S., & J., S. (2018). Rare earth doped semiconductor nanomaterials and its photocatalytic and antimicrobial activities. Journal of Environmental Chemical Engineering, 6(4), 3907–3917. https://doi.org/10.1016/j.jece.2018.05.046.

[36] Maddahi, P., Shahtahmasebi, N., Kompany, A., Mashreghi, M., Safaee, S., & Roozban, F. (2014). Effect of doping on structural and optical properties of ZnO nanoparticles: Study of antibacterial properties. Materials Science-Poland, 32(2), 130–135. https://doi.org/10.2478/s13536-013-0181-x.

[37] Magdalane, C. M., Priyadharsini, G. M. A., Kaviyarasu, K., Jothi, A. I., & Simiyon, G. G. (2021). Synthesis and characterization of TiO2 doped cobalt ferrite nanoparticles via microwave method: Investigation of photocatalytic performance of congo red degradation dye. Surfaces and Interfaces, 25, 101296. https://doi.org/10.1016/j.surfin.2021.101296.

[38] Manoharan, C., Pavithra, G., Dhanapandian, S., & Dhamodharan, P. (2015). Effect of In doping on the properties and antibacterial activity of ZnO films prepared by spray pyrolysis. Spectrochimica Acta Part A: Molecular and Biomolecular Spectroscopy, 149, 793–799. https://doi.org/10.1016/j.saa.2015.05.019.

[39] Maria Bernadette Leena, A., & Raji, K. (2019). Room temperature ferromagnetism in fe doped cds and cobalt doped cds nano particles. Materials Today: Proceedings, 8, 362–370. https://doi.org/10.1016/j.matpr.2019.02.124.

[40] Menanteau-Ledouble, S., Krauss, I., Santos, G., Fibi, S., Weber, B., & El-Matbouli, M. (2015). Effect of a phytogenic feed additive on the susceptibility of Onchorhynchus mykiss to Aeromonas salmonicida. Diseases of Aquatic Organisms, 115(1), 57–66. https://doi.org/10.3354/dao02875.

[41] Mondal, S., Bhattacharya, S., & Mitra, P. (2013). Structural, morphological, and lpg sensing properties of al-doped zno thin film prepared by silar. Advances in Materials Science and Engineering, 2013, 1–6. https://doi.org/10.1155/2013/382380.

[42] Mote, V. D., Purushotham, Y., Shinde, R. S., Salunke, S. D., & Dole, B. N. (2015). Structural, optical and antibacterial properties of yttriumdoped ZnO nanoparticles. Cerâmica, 61(360), 457–461. https://doi.org/10.1590/0366-69132015613601932.

[43] Nam, W. H., Lim, Y. S., Choi, S.-M., Seo, W.-S., & Lee, J. Y. (2012). High-temperature charge transport and thermoelectric properties of a degenerately Al-doped ZnO nanocomposite. Journal of Materials Chemistry, 22(29), 14633. https://doi.org/10.1039/c2jm31763j.

[44] Oh, B.-Y., Jeong, M.-C., Moon, T.-H., Lee, W., Myoung, J.-M., Hwang, J.-Y., & Seo, D.-S. (2006). Transparent conductive Al-doped ZnO films for liquid crystal displays. Journal of Applied Physics, 99(12), 124505. https://doi.org/10.1063/1.2206417.

[45] Onuegbu, C. U., Aggarwal, A., & Singh, N. B. (2018). Zno nanoparticles as feed supplement on growth performance of cultured african catfish fingerlings. JSIR Vol.77(04) [April 2018]. http://nopr.niscpr.res.in/handle/123456789/44151.

[46] Osonga, F. J., Kalra, S., Miller, R. M., Isika, D., & Sadik, O. A. (2020). Synthesis, characterization and antifungal activities of eco-friendly palladium nanoparticles. RSC Advances, 10(10), 5894–5904. https://doi.org/10.1039/C9RA07800B.

[47] Patterson, A. L. (1939). The scherrer formula for x-ray particle size determination. Physical Review, 56(10), 978–982. https://doi.org/10.1103/PhysRev.56.978.

[48] Raghupathi, K. R., Koodali, R. T., & Manna, A. C. (2011). Size-dependent bacterial growth inhibition and mechanism of antibacterial activity of zinc oxide nanoparticles. Langmuir, 27(7), 4020–4028. https://doi.org/10.1021/la104825u.

[49] Raja, K., Ramesh, P. S., & Geetha, D. (2014). Structural, FTIR and photoluminescence studies of Fe doped ZnO nanopowder by co-precipitation method. Spectrochimica Acta Part A: Molecular and Biomolecular Spectroscopy, 131, 183–188. https://doi.org/10.1016/j.saa.2014.03.047.

[50] Rao, T. P., Kumar, M. C. S., Angayarkanni, S. A., & Ashok, M. (2009). Effect of stress on optical band gap of ZnO thin films with substrate temperature by spray pyrolysis. Journal of Alloys and Compounds, 485(1–2), 413–417. https://doi.org/10.1016/j.jallcom.2009.05.116.

[51] Ravichandran, K., Karthika, K., Sakthivel, B., Jabena Begum, N., Snega, S., Swaminathan, K., & Senthamilselvi, V. (2014). Tuning the combined magnetic and antibacterial properties of ZnO nanopowders through Mn doping for biomedical applications. Journal of Magnetism and Magnetic Materials, 358–359, 50–55. https://doi.org/10.1016/j.jmmm.2014.01.008.

[52] Ravichandran, K., Snega, S., Jabena Begum, N., Swaminathan, K., Sakthivel, B., Rene Christena, L., Chandramohan, G., & Ochiai, S. (2014). Enhancement in the antibacterial efficiency of ZnO nanopowders by tuning the shape of the nanograins through fluorine

doping. Superlattices and Microstructures, 69, 17–28. https://doi.org/10.1016/j.spmi.2014.01.020.

[53] Repelin, Y., Proust, C., Husson, E., & Beny, J. M. (1995). Vibrational spectroscopy of the c-form of yttrium sesquioxide. Journal of Solid State Chemistry, 118(1), 163–169. https://doi.org/10.1006/jssc.1995.1326.

[54] Salah, N., Habib, Khan, Memic, Azam, Al-Hamedi, Zahed, & Habib. (2011). High-energy ball milling technique for ZnO nanoparticles as antibacterial material. International Journal of Nanomedicine, 863. https://doi.org/10.2147/IJN.S18267.

[55] Salaken, S. M., Farzana, E., & Podder, J. (2013). Effect of Fe-doping on the structural and optical properties of ZnO thin films prepared by spray pyrolysis. Journal of Semiconductors, 34(7), 073003. https://doi.org/10.1088/1674-4926/34/7/073003.

[56] Saliani, M., Jalal, R., & Kafshadre. Goharshadi, E. (2015). Effects of ph and temperature on antibacterial activity of zinc oxide nanofluid against e. Colio157:h7 and staphylococcus aureus. Jundishapur Journal of Microbiology, 8(2). https://doi.org/10.5812/jjm.17115.

[57] Sato, T., Imaeda, S., & Sato, K. (1988). Thermal transformation of yttrium hydroxides to yttrium oxides. Thermochimica Acta, 133, 79–85. https://doi.org/10.1016/0040-6031(88)87140-5.

[58] Sawai, J. (2003). Quantitative evaluation of antibacterial activities of metallic oxide powders (Zno, mgo and cao) by conductimetric assay. Journal of Microbiological Methods, 54(2), 177–182. https://doi.org/10.1016/S0167-7012(03)00037-X.

[59] Scherrer, P.,Göttinger Nachrichten. (1918). Math. Phys. 2, 98–100. https://doi:org/ 10.4236/opj.2019.911016.

[60] Shaalan, M. I., El-Mahdy, M. M., Theiner, S., El-Matbouli, M., & Saleh, M. (2017). In vitro assessment of the antimicrobial activity of silver and zinc oxide nanoparticles against fish pathogens. Acta Veterinaria Scandinavica, 59(1), 49. https://doi.org/10.1186/s13028-017-0317-9.

[61] Shaalan, M. I., El-Mahdy, M. M., Theiner, S., El-Matbouli, M., & Saleh, M. (2017). In vitro assessment of the antimicrobial activity of silver and zinc oxide nanoparticles against fish pathogens. Acta Veterinaria Scandinavica, 59(1), 49. https://doi.org/10.1186/s13028-017-0317-9

[62] Shaalan, M., Saleh, M., El-Mahdy, M., & El-Matbouli, M. (2016). Recent progress in applications of nanoparticles in fish medicine: A review. Nanomedicine: Nanotechnology, Biology and Medicine, 12(3), 701–710. https://doi.org/10.1016/j.nano.2015.11.005.

[63] Shan, W., Walukiewicz, W., Ager, J. W., Yu, K. M., Yuan, H. B., Xin, H. P., Cantwell, G., & Song, J. J. (2005). Nature of room-temperature photoluminescence in ZnO. Applied Physics Letters, 86(19), 191911. https://doi.org/10.1063/1.1923757.

[64] Sharma, D., Rajput, J., Kaith, B. S., Kaur, M., & Sharma, S. (2010). Synthesis of ZnO nanoparticles and study of their antibacterial and antifungal properties. Thin Solid Films, 519(3), 1224–1229. https://doi.org/10.1016/j.tsf.2010.08.073.

[65] Shinde, V. R., Gujar, T. P., Lokhande, C. D., Mane, R. S., & Han, S.-H. (2006). Mn doped and undoped ZnO films: A comparative structural, optical and electrical properties study. Materials Chemistry and Physics, 96(2–3), 326–330. https://doi.org/10.1016/j.matchemphys.2005.07.045.

[66] Singh, R., & Lillard, J. W. (2009). Nanoparticle-based targeted drug delivery. Experimental and Molecular Pathology, 86(3), 215–223. https://doi.org/10.1016/j.yexmp.2008.12.004.
[67] Sirelkhatim, A., Mahmud, S., Seeni, A., Kaus, N. H. M., Ann, L. C., Bakhori, S. K. M., Hasan, H., & Mohamad, D. (2015). Review on zinc oxide nanoparticles: Antibacterial activity and toxicity mechanism. Nano-Micro Letters, 7(3), 219–242. https://doi.org/10.1007/s40820-015-0040-x.
[68] Srinivasulu, T., Saritha, K., & Reddy, K. T. R. (2017). Synthesis and characterization of Fe-doped ZnO thin films deposited by chemical spray pyrolysis. Modern Electronic Materials, 3(2), 76–85. https://doi.org/10.1016/j.moem.2017.07.001.
[69] Suresh, D., Shobharani, R. M., Nethravathi, P. C., Pavan Kumar, M. A., Nagabhushana, H., & Sharma, S. C. (2015). Artocarpus gomezianus aided green synthesis of ZnO nanoparticles: Luminescence, photocatalytic and antioxidant properties. Spectrochimica Acta Part A: Molecular and Biomolecular Spectroscopy, 141, 128–134. https://doi.org/10.1016/j.saa.2015.01.048.
[70] Suvith, V. S., & Philip, D. (2014). Catalytic degradation of methylene blue using biosynthesized gold and silver nanoparticles. Spectrochimica Acta Part A: Molecular and Biomolecular Spectroscopy, 118, 526–532. https://doi.org/10.1016/j.saa.2013.09.016.
[71] Swain, P., Nayak, S. K., Sasmal, A., Behera, T., Barik, S. K., Swain, S. K., Mishra, S. S., Sen, A. K., Das, J. K., & Jayasankar, P. (2014). Antimicrobial activity of metal based nanoparticles against microbes associated with diseases in aquaculture. World Journal of Microbiology and Biotechnology, 30(9), 2491–2502. https://doi.org/10.1007/s11274-014-1674-4.
[72] Tam, K. H., Djurišić, A. B., Chan, C. M. N., Xi, Y. Y., Tse, C. W., Leung, Y. H., Chan, W. K., Leung, F. C. C., & Au, D. W. T. (2008). Antibacterial activity of ZnO nanorods prepared by a hydrothermal method. Thin Solid Films, 516(18), 6167–6174. https://doi.org/10.1016/j.tsf.2007.11.081
[73] Thirumoorthi, M., & Thomas Joseph Prakash, J. (2015). Structural, morphological characteristics and optical properties of Y doped ZnO thin films by sol–gel spin coating method. Superlattices and Microstructures, 85, 237–247. https://doi.org/10.1016/j.spmi.2015.05.005.
[74] Thirumoorthi, M., Dhavud, S. S., Ganesh, V., Al Abdulaal, T. H., Yahia, I. S., & Deivatamil, D. (2022). High responsivity n-ZnO/p-CuO heterojunction thin film synthesised by low-cost SILAR method for photodiode applications. Optical Materials, 128, 112410. https://doi.org/10.1016/j.optmat.2022.112410.
[75] Thongsuriwong, K., Amornpitoksuk, P., & Suwanboon, S. (2012). Photocatalytic and antibacterial activities of Ag-doped ZnO thin films prepared by a sol–gel dip-coating method. Journal of Sol-Gel Science and Technology, 62(3), 304–312. https://doi.org/10.1007/s10971-012-2725-7.
[76] Umar, A., Kumar, R., Kumar, G., Algarni, H., & Kim, S. H. (2015). Effect of annealing temperature on the properties and photocatalytic efficiencies of ZnO nanoparticles. Journal of Alloys and Compounds, 648, 46–52. https://doi.org/10.1016/j.jallcom.2015.04.236.
[77] Vasanthi, M., Ravichandran, K., Jabena Begum, N., Muruganantham, G., Snega, S., Panneerselvam, A., & Kavitha, P. (2013). Influence of Sn doping level on antibacterial

activity and certain physical properties of ZnO films deposited using a simplified spray pyrolysis technique. Superlattices and Microstructures, 55, 180–190. https://doi.org/10.1016/j.spmi.2012.12.011.

[78] Wang, J., Wang, A., & Wang, W.-X. (2017). Evaluation of nano-ZnOs as a novel Zn source for marine fish: Importance of digestive physiology. Nanotoxicology, 11(8), 1026–1039. https://doi.org/10.1080/17435390.2017.1388865.

[79] Webster, T. J., & Seil, I. (2012). Antimicrobial applications of nanotechnology: Methods and literature. International Journal of Nanomedicine, 2767. https://doi.org/10.2147/IJN.S24805.

[80] Yu, Q., Fu, W., Yu, C., Yang, H., Wei, R., Sui, Y., Liu, S., Liu, Z., Li, M., Wang, G., Shao, C., Liu, Y., & Zou, G. (2007). Structural, electrical and optical properties of yttrium-doped ZnO thin films prepared by sol–gel method. Journal of Physics D: Applied Physics, 40(18), 5592–5597. https://doi.org/10.1088/0022-3727/40/18/014.

[81] Yu, Q., Yang, H., Fu, W., Chang, L., Xu, J., Yu, C., Wei, R., Du, K., Zhu, H., Li, M., & Zou, G. (2007). Transparent conducting yttrium-doped ZnO thin films deposited by sol–gel method. Thin Solid Films, 515(7–8), 3840–3843. https://doi.org/10.1016/j.tsf.2006.10.077.

[82] Yun'an Qing, Lin Cheng, Ruiyan Li, Guancong Liu, Yanbo Zhang, Xiongfeng Tang, Jincheng Wang, He Liu & Yanguo Qin (2018), Potential antibacterial mechanism of silver nanoparticles and the optimization of orthopedic implants by advanced modification technologies, Int Journal of Nanomedicine, 3311-3327, https://doi.org/ 10.2147/IJN.S165125